Hydraulic Conductivity Measurement from On-the-Fly uCPT Sounding and from VisCPT

Dae Sung Lee[1]; Derek Elsworth[2]; and Roman Hryciw[3]

Abstract: Detailed profiles of hydraulic conductivity are recovered from the deployment of direct-push permeameters at the Geohydrologic Experimental and Monitoring Site, Kansas. Measurements with thin tapered tips, and with standard cone penetration test (uCPT) tips, show only minor differences, suggesting that tip-local disturbance effects are small, and that routine uCPT measurements are therefore representative of pristine conditions. Permeameter measurements are correlated against closely deployed uCPT measurements, estimates of hydraulic conductivity from uCPT sounding correlations, and from grain size correlations derived from both vision CPT (VisCPT) and from cone metrics. On-the-fly evaluations of hydraulic conductivity require that the tip-local pressure field is both steady and partially drained. Continuous penetration is shown to yield pore pressures sufficiently close to steady to enable conductivities to be directly determined. Cone metrics of cone resistance, sleeve friction, and pore pressure ratio are shown to be sufficient to discriminate between partially drained and undrained behavior, and therefore to define the permissible regime where conductivities may be determined from uCPT sounding data. Estimates of hydraulic conductivities from uCPT sounding data are shown to correlate with independently measured magnitudes of hydraulic conductivity recovered using the permeameter tests. However, most of hydraulic conductivities from the permeameter tests (4.5 cm length screen) are underpredicted, suggesting that storage effects, the inability to reach a steady state, or the effects of dilation may influence the response. Profiles of hydraulic conductivities evaluated from the on-the-fly method also correlate well with the permeameter measurements. Predictions from soil classification and from VisCPT methods are also capable of estimating conductivities, with soil classifications giving the closest correlations of these two for this particular suite of data.

DOI: 10.1061/(ASCE)1090-0241(2008)134:12(1720)

CE Database subject headings: Soil permeability; Hydraulic conductivity; Cone penetration tests; Saturated soils; Measurement.

Introduction

Cone penetration testing (uCPT) is a rapid and robust method for determining the mechanical and transport properties of soils, and the distribution of contaminants in the ground (Mitchell and Brandon 1998). In a standard uCPT test, a conically tipped probe (penetrometer) is pushed into the ground at a constant penetration rate of 2 cm/s. Depth-continuous measurements are made of the resistance to penetration, q_t, of the frictional resistance of a trailing sleeve, f_s, and of the penetration-induced pore-fluid pressure, $p(u_2)$, immediately above the cone tip (Lunne et al. 1997). The vision cone penetration test (VisCPT) (Raschke and Hryciw 1997; Hryciw et al. 1998) significantly improves the resolving capabilities of the uCPT by providing a continuous visual record of the penetration log. Current uCPT methods for determining hydraulic conductivity in the soil are primarily based on the dissipation test (Robertson et al. 1992; Burns and Mayne 1998), which involves temporarily suspending penetrometer advance and monitoring the dissipation of the penetration-induced pore pressures. Dissipation tests are complemented by other direct-push methods of deploying permeameters, and then conducting, slug tests (Butler 2002; 2005), constant-head injection tests (CHIT) (Cardenas and Zlotnik 2003), and direct-push permeameter tests (DPP) (Butler and Dietrich 2004). Although capable of recovering accurate measurements of hydraulic conductivity profiles with depth, they do not allow the concurrent measurement of traditional cone metrics, nor visual profiling with depth, and are typically laborious and time consuming.

The pore pressures generated during uCPT penetration are a function of the hydraulic conductivity of the surrounding medium. Thus, measurements of pore pressures and other uCPT parameters could potentially be the basis of a useful method of determining hydraulic conductivity, on-the-fly, i.e., without the need to suspend advance and waiting to perform a dissipation test (Elsworth 1993). Approximate steady solutions for the pore pressures developed around an advancing penetrometer enable hydraulic conductivity to be determined (Elsworth and Lee 2005), and the limits for which these correlations are appropriate may be defined (Elsworth and Lee 2007). Despite the utility of such correlations between cone metrics and hydraulic conductivity, a lack of uCPT soundings, colocated with independent in situ measurements of hydraulic conductivity, has made it difficult to verify the accuracy and value of such an approach. This study reports unusually well-resolved measurements of hydraulic conductivity gathered from newly developed in situ permeameters, colocated with uCPT measurements and VisCPT observations. These measurements examine the potential role of tip-local disturbance, and

[1]Senior Researcher, Petroleum and Marine Resources Division, Korea Institute of Geoscience and Mineral Resources, Daejeon, Korea (corresponding author). E-mail: leeds@rock25t.kigam.re.kr

[2]Professor, Dept. of Energy and Mineral Engineering, Pennsylvania State Univ., University Park, PA 16802-5000. E-mail: elsworth@psu.edu

[3]Professor, Dept. of Civil and Environmental Engineering, Univ. of Michigan, Ann Arbor, MI 48109-2125. E-mail: romanh@umich.edu

Note. Discussion open until May 1, 2009. Separate discussions must be submitted for individual papers. The manuscript for this paper was submitted for review and possible publication on August 28, 2006; approved on May 14, 2007. This paper is part of the ***Journal of Geotechnical and Geoenvironmental Engineering***, Vol. 134, No. 12, December 1, 2008. ©ASCE, ISSN 1090-0241/2008/12-1720–1729/$25.00.

Downloaded 15 Nov 2008 to 128.118.16.83. Redistribution subject to ASCE license or copyright; see http://pubs.asce.org/copyright

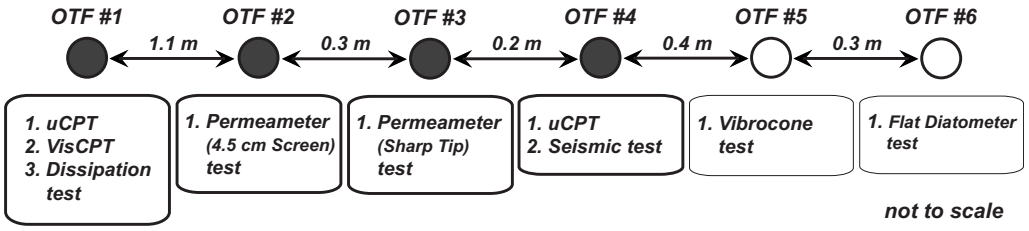

Fig. 1. Area view of profile locations and plan of in situ test holes [Geohydrologic Experimental and Monitoring Site, Kansas]

independently examine the relative accuracy of hydraulic conductivity determinations derived from soil classification (Robertson 1990), from visual VisCPT measurements, and from on-the-fly measurements of pore pressures.

Field Site

This work was performed at the Geohydrologic Experimental and Monitoring Site (GEMS). This is a research site of the Kansas Geological Survey located in the floodplain of the Kansas River just north of Lawrence, Kansas, in the central portion of the United States. GEMS has been the site of extensive research on flow and transport in heterogeneous formations (Bohling 1999; Butler et al. 1999a,b; Bohling et al. 2002; Butler 2002, 2005; McElwee et al. 1991; McCall et al. 2002; Schulmeister et al. 2003a,b; Sellwood et al. 2005). These previous studies enabled the techniques discussed here to be evaluated in a relatively controlled field setting. The shallow subsurface at GEMS consists of 22 m of normally consolidated Holocene sediments of Kansas River alluvium that overlie and are adjacent to materials of Pennsylvanian and the late Pleistocene ages, respectively. Fig. 2 displays a cross-sectional view of the shallow subsurface with electrical conductivity logging data obtained from a direct-push probe (Butler et al. 1999a), and a geologic interpretation from core and logging data. As shown in that figure, the heterogeneous alluvium at GEMS consists of 11.5 m of primarily clay and silt overlying 10.7 m of sand and gravel, which is hydraulically confined by the overlying materials. The subarea of the GEMS site used in this work is depicted in Fig. 1. This figure displays the location and plan of the in situ tests and test holes. The uCPT, VisCPT, and in situ permeameter soundings were performed as part of the work reported here.

Methods

Profiles of hydraulic conductivities determined from in situ permeameters were compared with independently measured magnitudes determined from correlations with grain size distributions, with soil classifications, and from pore pressures determined on-the-fly. The six soundings included continuous uCPT (OTF#4), VisCPT (OTF#1), dissipation tests (OTF#1), and permeameter tests (OTF#2&3), deployments, supplemented by seismic (OTF#4), vibrocone (OTF#5), and dilatometer tests (OTF#6) as noted in Fig. 1. The latter three are unused in this analysis. These different methods for evaluating hydraulic conductivities are documented in the following section.

In Situ Permeameter Tests

An in situ permeameter was fabricated and then deployed to obtain independent evaluations of in situ hydraulic conductivities along the cone sounding path. To quantify the effects of disturbance in the testing zone, tips of variable diameter ($2a=3.7$ and 1.2 cm) and taper were developed, as illustrated in Fig. 3. The sharp cone tip is similar in form to piezoprobes (Ostermeier et al. 2001; Whittle et al. 2001; Dejong et al. 2003), comprising a thin advance probe extending 0.15 m (25 radii) beyond the penetrometer tip, as shown in Fig. 3(b). Screens were fabricated with a slot size of 0.3 mm, corresponding to a No. 10 screen, at diameters and lengths of 3.7 and 4.5 cm for the large tip, and of 1.2 and 1.2 cm, for the sharp tip. These permeameter tips were deployed in two parallel soundings separated laterally by 0.2 m [OTF #3; 1.2 cm length screen (sharp tip)] and 0.5 m (OTF #2; 4.5 cm length screen) from the uCPT test hole (OTF #4), respectively, as illustrated in Fig. 1. The in situ permeameter test involved pressurizing the water column in the above-ground reservoir via compressed nitrogen gas, and measuring the rate of reservoir discharge under constant pressure. Water discharge into the formation was through the perforated screen (Fig. 3). Flow rate, Q, was measured manually as a volume discharged over a measured time, with the test initiated by rapidly pressurizing the water column. Staged measurements were made in two parallel incremented advances using the fabricated probes. In situ permeameter tests were completed in the upper 12 m at intervals of 1.0 m, and below 12 m at intervals of 0.25 m.

Screen clogging was avoided by pressurizing the penetrometer

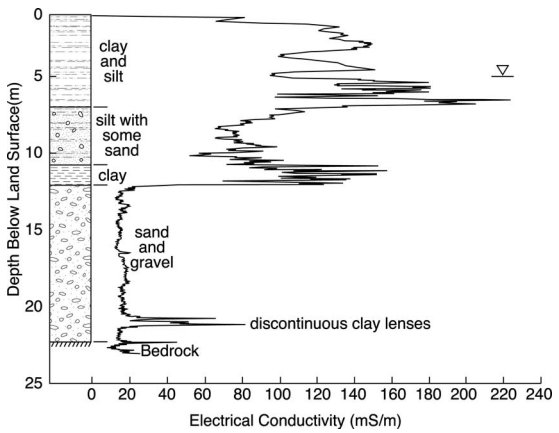

Fig. 2. Generalized GEMS stratigraphy with electrical conductivity log from G4SGPA (after Butler et al. 1999a; inverted triangle marks position of water table, head in sand and gravel interval is approximately 1 m lower)

Downloaded 15 Nov 2008 to 128.118.16.83. Redistribution subject to ASCE license or copyright; see http://pubs.asce.org/copyright

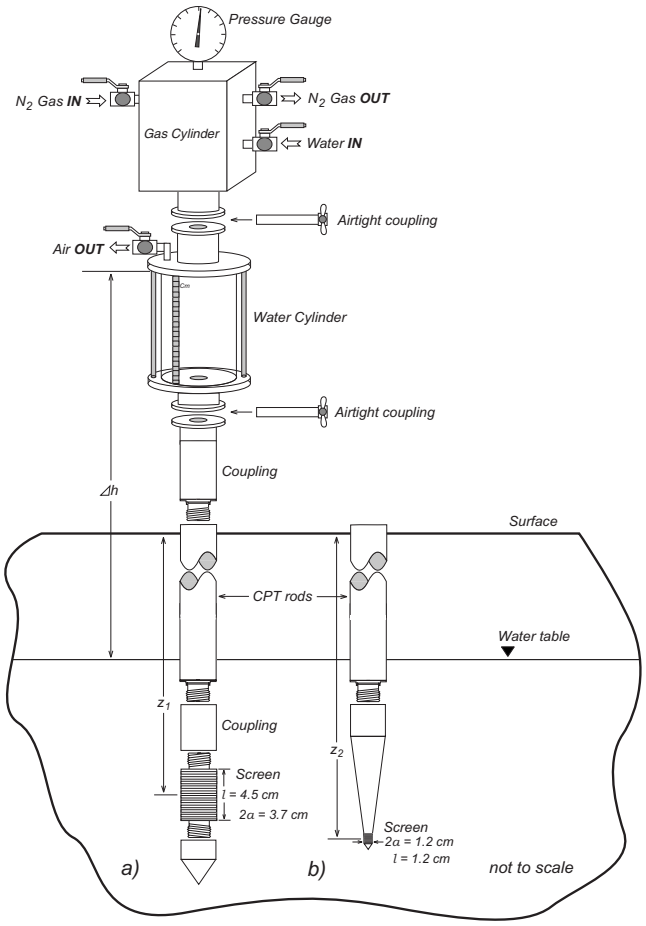

Fig. 3. In situ permeameter tests using two different diameter probe tips [(a) $2a=3.7$ cm; (b) 1.2 cm], injection fluids through fabricated screens

column and tip, prior to advance. Penetration through the upper 6 m was by preadvance with a solid-tipped cone, withdrawal, and then secondary advance of the permeameter tip through the remnant hole. To confirm free-flowing conditions at the tip outflow screen, multiple in situ permeameter tests were performed at each arrest depth using incremented pressures. The linearity between head drop, Δh, and flow rate, Q, was confirmed, with excess heads limited to avoid hydraulic fracturing of the soil.

Hydraulic conductivity magnitudes, K, were recovered from the applied excess head, Δh, and measured volumetric flow rate, Q, through the spherical form of Darcy's law

$$K = \frac{Q}{4\pi \Delta h a_s} \tag{1}$$

where a_s=effective radius of the spherical injection zone. This is the radius of a sphere with a specific surface area equal to the flowing area of the cylindrical screen with an impervious top and bottom. The equivalent radius is

$$a_s = \sqrt{\tfrac{1}{2} a l} \tag{2}$$

where a=radius of the screen; and l=length of the screen. In addition to this characterization, the appropriateness of the equivalent radius was checked against the results of calibration chamber tests. Permeameter tests were conducted in two different geometries ($H \times D = 21$ cm $\times$ 10 cm for the sharp tip and $H \times D = 22$ cm $\times$ 26 cm for the large 4.5 cm length screen) for known hydraulic conductivities. Calibration chamber measured conductivities were within factors of 1.09 (sharp permeameter) and 1.21 (4.5 cm permeameter) of mean measured hydraulic conductivity magnitudes of the soil specimen. Correspondingly, the measured magnitudes of in situ hydraulic conductivity are used with confidence.

Soil Classifications (Vision Cone Penetration Testing)

The uCPT metrics may be used to determine soil characteristics (Douglas and Olsen 1981; Robertson et al. 1986) based on grain-size distributions. The metrics of pore pressure ratio, B_q, friction ratio, F_r, and cone resistance, Q_t, may be used to define soil type, and the hydraulic conductivity of the soil may be approximated from its type or related grain size distribution (Robertson 1990), as shown in Table 1. As an alternative to the use of traditional cone metrics, the VisCPT may be used to directly capture a continuous real-time image of the soil. A total of 1,500 images are captured per meter of advance (Hryciw et al. 2003), with this completed along one cone sounding (OTF #1). Through image analysis, the VisCPT is used to define the soil grain size, with hydraulic conductivities computed using the Hazen formula (Hazen 1930) for sand (below a depth 12 m) [Eq. (3)], based on the diameter of the soil particles (Hryciw et al. 2003) (Table 1)

Table 1. Hydraulic Conductivity Predictions from Soil Classifications (Robertson 1990 and VisCPT)

	Soil classification (Robertson 1990; Fetter 1998)		Soil classification (VisCPT)		
Depth (m)	Soil classification	Presumed hydraulic conductivity (m/s)	Average number of pixels per (soil particle) diameter (PPD) (pixels/diameter)	Diameter of soil particle (D) (mm)	Presumed hydraulic conductivity (m/s)
12.7	Sand	10^{-5}–10^{-4}	10	0.20	4.8×10^{-4}
13.7	Gravelly sand and sand	10^{-5}–10^{-3}	12	0.24	6.9×10^{-4}
14.7	Sand	10^{-5}–10^{-4}	15	0.29	1.1×10^{-3}
15.7	Sand	10^{-5}–10^{-4}	18	0.35	1.6×10^{-3}
16.7	Sand and silt sand	10^{-6}–10^{-4}	28	0.55	3.8×10^{-3}
17.7	Sand	10^{-5}–10^{-4}	26	0.51	3.3×10^{-3}
18.7	Sand	10^{-5}–10^{-4}	9	0.18	3.9×10^{-4}

Downloaded 15 Nov 2008 to 128.118.16.83. Redistribution subject to ASCE license or copyright; see http://pubs.asce.org/copyright

$$K(\text{cm/s}) = cD^2 \tag{3}$$

where c=constant (c=1.25 in this analysis); and D=effective size (mm), approximately 0.1 and 3.0 mm. The camera for the VisCPT record images at a magnification of 51 pixels/mm. The average number of pixels per (soil particle) diameter (PPD) was used to represent the relative size of soil particles within an image. The diameter of the soil particles can then be computed from the magnification (51 pixels/mm) and the number of PPD, as shown in Table 1, using the following equation (Shin and Hryciw 2004):

$$D(\text{mm/diameter}) = \frac{\text{PPD(pixels/diameter)}}{\text{magnification level(pixels/mm)}} \tag{4}$$

These characterizations are later compared with independently measured magnitudes of hydraulic conductivity, recovered from the permeameter tests.

On-the-Fly Method

In a uCPT profile, pore fluid pressure, p, cone resistance, q_t, and sleeve friction, f_s, are measured continuously with depth. By convention, these three quantities are defined in dimensionless form as the pore pressure ratio, B_q, cone resistance, Q_t, and sleeve friction, F_r

$$B_q = \frac{p - p_s}{q_t - \sigma_{v0}}; \quad Q_t = \frac{q_t - \sigma_{v0}}{\sigma'_{v0}}; \quad F_r = \frac{f_s}{q_t - \sigma_{v0}} \tag{5}$$

where q_t=corrected cone resistance; f_s=sleeve friction defined in units of stress; σ_{v0}=initial in situ vertical stress, and the prime denotes effective stress.

Changes in pore pressure resulting from the advance of the penetrometer may be approximated by a moving volumetric dislocation of finite size migrating within a saturated porous medium (Elsworth 1990; Elsworth and Lee 2005). The steady fluid pressure distribution that develops around the cone can be considered equivalent to the pressure field produced by the continuous injection of fluid into the porous medium surrounding a spherical cavity. This constant injection of fluid volume per unit time is equivalent to the product of penetrometer advance rate per unit time and penetrometer cross-sectional area. For a penetrometer of diameter $2a$ advanced at rate U, the fluid volume injected per unit time (dV) is equal to $\pi a^2 U$. This flux is injected on the spherical shell of the cavity with the condition of no change in fluid pressure in the far field, or $p=p_s$. This flux dissipates roughly spherically, and there is little fluid storage (no storage effect is considered) in the system. Solving the spherically symmetric flow problem yields the following relationship (Elsworth and Lee 2005):

$$p - p_s = \frac{\gamma_w}{4\pi Ka} dV = \frac{Ua\gamma_w}{4K} \tag{6}$$

where p_s=hydrostatic pore fluid pressure, relative to the pressure measured at the penetrometer face; a=radius of the penetrometer; and U=penetration rate. Eq. (6) represents the pressure induced by fluid injection across the interior surface of the spherical shell at a rate equivalent to the displacement volume per unit time of the penetrometer. This simplified solution is unable to discriminate between pore pressures measured on the tip, shoulder, or shaft, as all are represented on the idealized geometry of the spherical surface.

An expression for hydraulic conductivity in terms of these dimensionless parameters can be obtained by manipulating Eq. (6). The penetration-induced excess pore pressure, $p-p_s$, can be normalized by the initial vertical effective stress (Elsworth and Lee 2005)

$$\frac{p - p_s}{\sigma'_{v0}} = \frac{Ua\gamma_w}{4K\sigma'_{v0}} = \frac{1}{K_D} \tag{7}$$

where K_D=dimensionless hydraulic conductivity index ($K_D = (4K\sigma'_{v0})/(Ua\gamma_w)$). The ratio $(p-p_s)/\sigma'_{v0}$ can be expressed in terms of the cone metrics of Eq. (5) as

$$\frac{p - p_s}{\sigma'_{v0}} = \frac{p - p_s}{q_t - \sigma_{v0}} \frac{q_t - \sigma_{v0}}{\sigma'_{v0}} = B_q Q_t = \frac{1}{K_D} \tag{8}$$

This expression relates the pore pressure ratio, B_q, and cone resistance, Q_t, to the dimensionless hydraulic conductivity, K_D. Eq. (8) can be rearranged as

$$K_D = \frac{1}{B_q Q_t} \tag{9}$$

Eq. (9) can be used to develop cross plots of B_q and Q_t that can be contoured for K_D as shown in Fig. 4(a). If B_q and Q_t are known, hydraulic conductivity, K, can be estimated from the K_D values as shown in the figures. Cross plots of these three pairs of metrics, B_q-Q_t, F_r-Q_t, and B_q-F_r, are given in Fig. 4 for an assumed friction angle of 30°, medium loose sands (Elsworth and Lee 2005). Importantly, this observationally confirmed relation enables hydraulic conductivity to be recovered during active penetration without arresting penetration and waiting for the pore pressure to dissipate. Appropriate analyses are compared with independently measured hydraulic conductivity estimates from GEMS.

Observations

Direct-push permeameter tests allow highly reliable measurements of hydraulic conductivity to be recovered for the full vertical profile. These measurements are the most repeatable of the suite of tests considered here, and in this work are considered the control data. Hydraulic conductivities recovered from the in situ permeameter tests will be compared systematically with those predicted from uCPT on-the-fly, soil classification (Robertson 1990), and VisCPT methods.

In Situ Permeameter Measurements

Measurements of hydraulic conductivities from the deployment of the twin permeameters in parallel soundings are illustrated for the GEMS site in Fig. 5. Hydraulic conductivity measurements were observed to be in the range 10^{-6}–10^{-4} m/s, except in the clay and silt layer above 12 m depth where conductivities are in the range 10^{-9}–10^{-8} m/s [Fig. 5(a)]. Although the profiles are measured with different diameter probes, and therefore with anticipated different degrees of tip-local disturbance, they show largely similar results. Below the apparent sand and gravel layer at around ~14.5 m, the 4.5 cm length-screen permeameter-derived measurements of hydraulic conductivity are higher than the sharp permeameter measurements (except above 12 m) [Fig. 5(b)]. Importantly, these results suggest only a very minor influence of tip-local disturbance, and hence the feasibility of measuring hydraulic conductivity magnitudes from standard CPT tip configurations. These resulting, and independently measured hydraulic

Downloaded 15 Nov 2008 to 128.118.16.83. Redistribution subject to ASCE license or copyright; see http://pubs.asce.org/copyright

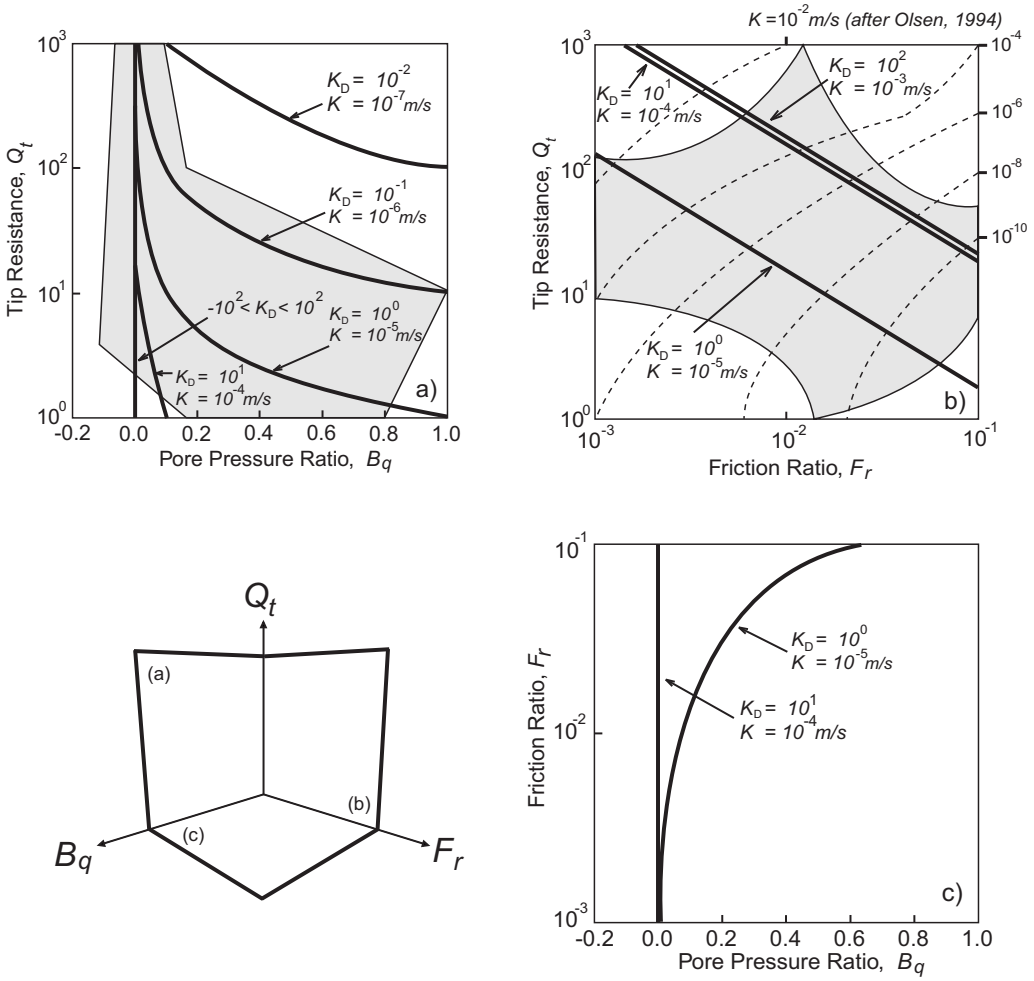

Fig. 4. Plots of: (a) $B_q - Q_t$; (b) $F_q - Q_t$; and (c) $B_q - F_t$ contoured for K_D for assumption of vertical stresses remain invariant (Elsworth and Lee 2005). Values of K are shown for standard 10 cm^2 cone with σ'_{v0}=100 kPa, and U=2 cm/s. Empirical results of Olsen (1994) are shown by dashed line in (b); and zero solid ranges of Robertson (1990) are shown shaded in (a) and (b).

conductivity profiles are used in the following section for comparison against alternate methods of determining conductivities.

On-the-Fly Method

A series of continuous uCPT soundings (OTF#4) are available from GEMS, as documented in Fig. 6. Penetration at the standard rate of 2 cm/s may result in the development of a steady pressure distribution around the cone tip, and this steady magnitude may be used to define the magnitude of the hydraulic conductivity. To be used in this manner, the generated pressures must be both steady state, and partially drained. They must not be undrained, as this index pore pressures to strength, rather than with hydraulic conductivity. These requirements are examined in the following section.

Steady State

The on-the-fly method of evaluating hydraulic conductivity requires that the pore fluid pressures that develop around the tip be at steady state. In this state, the steady pore pressure results from a balance between the rate of pore fluid generation (controlled by the mean strain rate imposed by the advancing cone) and the rate of pore pressure dissipation (controlled by the hydraulic conductivity). Two sets of sounding data (OTF #1 and OTF #4) are available to depths of ~19 m, and characteristic of different penetrometer-rod change-out characteristics. The first is completed with dissipation tests conducted at each new rod addition, and the second with continuous rod advance, as noted in Fig. 6. The first profile (OTF #1) is used to measure the hydrostatic pressure (p_s) distributions through the conduct of dissipation tests at eight different depths (Fig. 7). The depth of the water table is back-calculated to be at 6.0 m. The second excess pore pressure profile (OTF #4) records considerably higher excess pressures than the first profile, indicating that the first profile did not reach steady state. The steady excess pore pressure ($p - p_s$) that develops around the penetrometer tip may be directly linked to the hydraulic conductivity of the surrounding soil. Where pore pressure profile (OTF #1) is excluded, the continuous profiling of penetration-induced pore pressure (OTF #4) during steady penetration is used for estimation of on-the-fly hydraulic conductivity in the following section.

Undrained Response

The pore fluid pressures generated following standard uCPT sounding in materials ranging from clays to sands (OTF #4) exhibit both undrained and partially drained response. Since undrained response can only provide information on the tip-local failure conditions, it is important to be able to discriminate this response from the partially drained behavior that we use to

Downloaded 15 Nov 2008 to 128.118.16.83. Redistribution subject to ASCE license or copyright; see http://pubs.asce.org/copyright

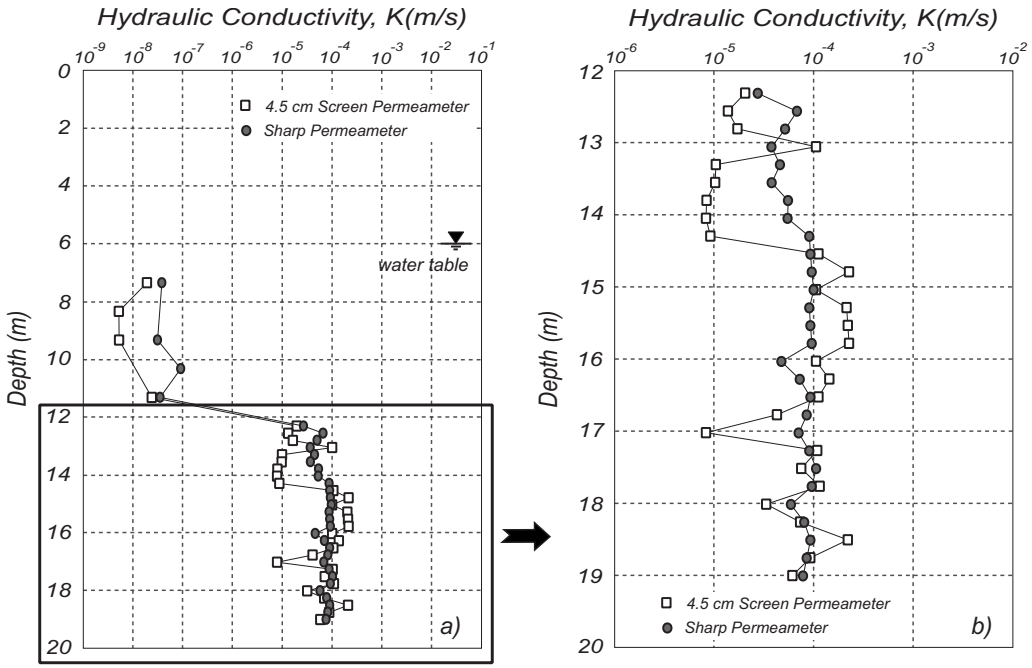

Fig. 5. Hydraulic conductivity measurements determined by in situ permeameter tests [4.5 cm screen (squares) and sharp tip (circles)] versus depth at GEMS, Kansas

define hydraulic conductivity. The transition from partially drained to undrained response may be defined in terms of the transition bounds as $B_qQ_t < 1.0 \sim 6.0$, $Q_tF_r < 0.3 \sim 0.7$, and $B_q/F_r < 4.0 \sim 8.0$ (Elsworth and Lee 2007), as illustrated in Fig. 8. These are represented on the standard plots of cone metrics as: (a) $B_q - Q_t$; (b) $F_r - Q_t$; and (c) $B_q - F_r$ in representing the uCPT data (OTF #4) from GEMS in Figs. 8(a–c). However, these data enable the bounds to be more tightly defined as $B_qQ_t < 0.2$, $F_rQ_t < 2.0$, and $F_r < 0.02$, and $B_q/F_r < 0.8$, respectively for the cone metrics (Fig. 8). Most of the presumed undrained data are not within the typical range of measurements, as $Q_t < 10^0$ [Fig. 8(b)] and $F_r > 10^{-1}$ [Fig. 8(c)]. These limits restrict the plausible range for partial drainage and only these partially drained data can be used to determine hydraulic conductivity

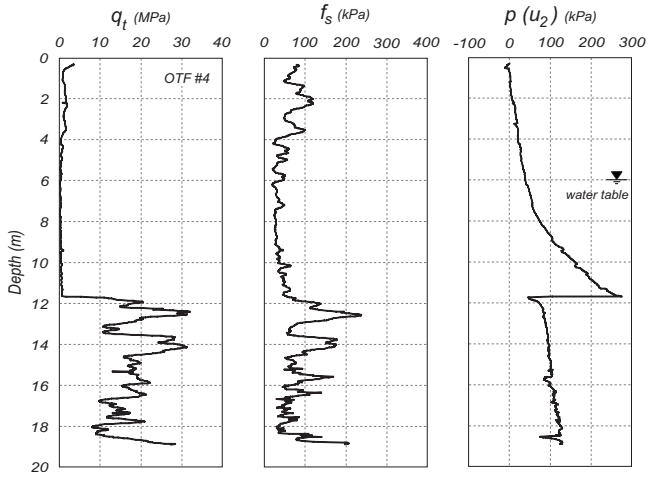

Fig. 6. Profile data from GEMS (OTF#4), defined by corrected cone resistance, q_t, sleeve friction, f_s, and pore pressure measured at cone shoulder (p, or u_2 in this analysis)

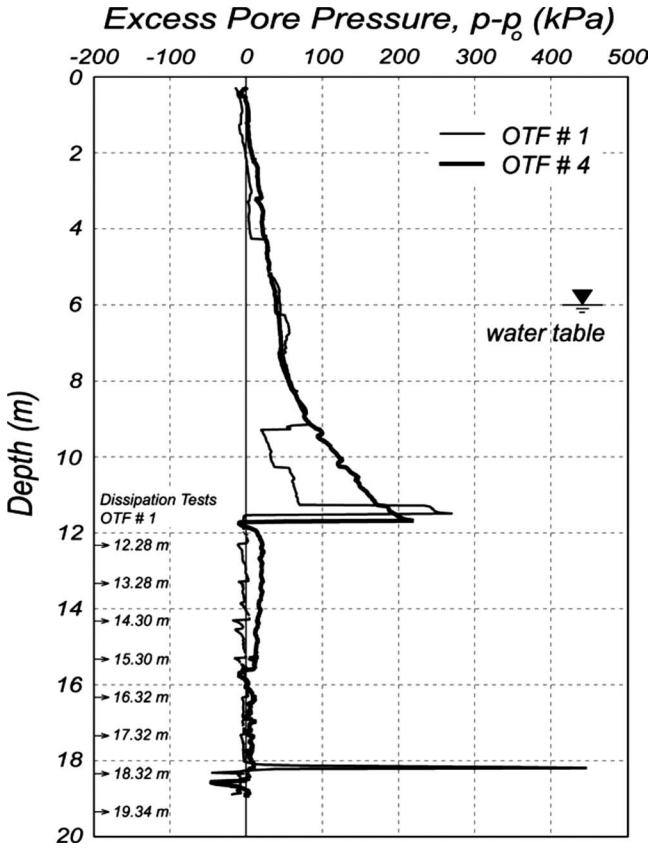

Fig. 7. Two excess pore pressure profiles: steady pore pressure were continuously recorded under steady penetration (OFT#4) and pore pressure, completed with arresting penetration for pore pressure dissipation tests (OFT#1)

Downloaded 15 Nov 2008 to 128.118.16.83. Redistribution subject to ASCE license or copyright; see http://pubs.asce.org/copyright

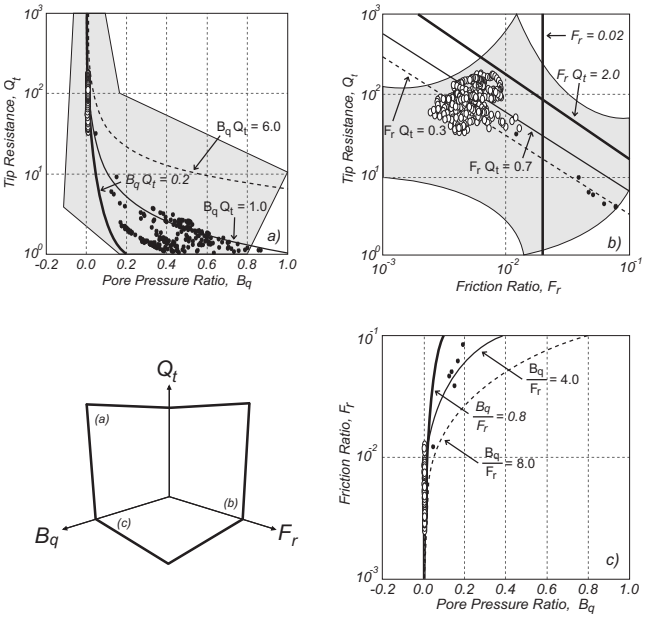

Fig. 8. Plots of cone metrics: (a) $B_q - Q_t$; (b) $Q_t - F_r$; and (c) $B_q - F_r$ with limits (range of transition given by solid and dashed lines) of undrained penetration identified. Shaded regions in (a) and (b) denote defined ranges of material types (Robertson 1990). Symbols denote data from undrained (black circles) and partially drained (white circles) response at GEMS.

magnitudes, on-the-fly. The limiting hydraulic conductivity predictions may be recovered for partially drained response using the relation $K_D = 1/B_q Q_t$, on-the-fly, where presumed undrained data, black circles in Fig. 8, are excluded. Hydraulic conductivity magnitudes may be defined in terms of the cone metric pair that indexes the transition from partially drained to undrained behavior. The hydraulic conductivities recovered from partially drained behavior are examined in the following section.

Prediction

Hydraulic conductivity may be recovered during steady uCPT penetration within the defined limits of partial drainage response. An alternative method of validating the on-the-fly method is to compare each magnitude of hydraulic conductivity measured by the in situ permeameter tests, using the two fabricated probe tips, with a paired prediction from $K_D = 1/B_q Q_t$ at an equivalent depth, as illustrated in Figs. 9(a and b). Hydraulic conductivities systematically recovered from $K_D = 1/B_q Q_t$ are compared with those measured from the permeameter tests. The in situ permeameter tests measure hydraulic conductivities, and these are converted to $K_D = (4K\sigma'_{v0})/(Ua\gamma_w)$, and are plotted on the horizontal ordinate. The permeameter measurements are assumed to represent the average hydraulic conductivity within an interval centered on the screen length (l=4.5 and 1.2 cm) (Fig. 3). For purposes of comparison, the harmonic average of the uCPT estimates is taken over the interval of the permeameter measurements (comprising 32 permeameter measurements). The presumed undrained data (the four permeameter measurements) are furthest from the theoretical relation, $K_D = 1/B_q Q_t$. Where undrained data are excluded, there are 28 remaining data points, representing partially drained uCPT estimates in the sand and gravel layers (below a depth of 12 m) (Elsworth and Lee 2007). The predictions recovered from the relation $K_D = 1/B_q Q_t$ yield consistent evaluations of hydraulic conductivity, as shown in Figs. 9(a and b). Most of the measurements from the permeameter tests (4.5 cm length screen) which satisfy the requirements of partial drainage, plot below the relation $K_D = 1/B_q Q_t$. This suggests that the induced pore pressures are smaller than those predicted by this relation, and that this undergeneration may result either from dilation around the tip, or from pore pressures being in a substeady state [Fig. 9(a)]. The hydraulic conductivities recovered for the sharp-tip permeameter are taken as most representative of the undisturbed hydraulic conductivities. The on-the-fly relationship is closest to the data as illustrated in Fig. 9(b). All data are within a one order-of-magnitude spread either side of the theoretical relation, $K_D = 1/B_q Q_t$.

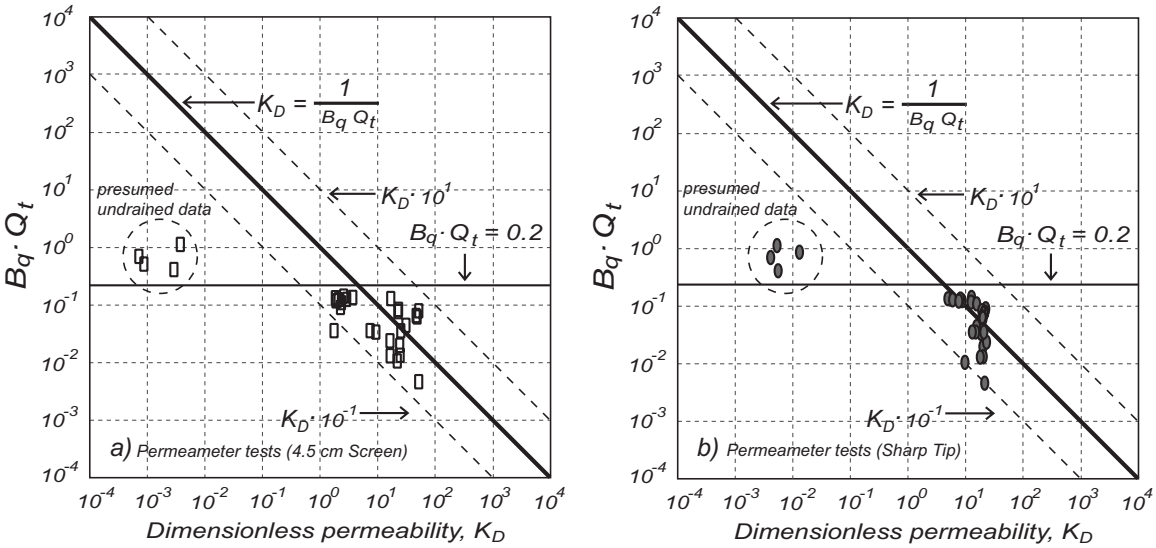

Fig. 9. (a) Selected hydraulic conductivity magnitudes determined from in situ permeameter test (4.5 cm length screen) adjacent to OTF# 4 (squares), compared with relation $K_D = 1/B_q Q_t$; (b) selected hydraulic conduvtity magnitudes determined from in situ permeameter test (sharp tip) adjacent to OTF# 4 (circles), compared with relation $K_D = 1/B_q Q_t$

Downloaded 15 Nov 2008 to 128.118.16.83. Redistribution subject to ASCE license or copyright; see http://pubs.asce.org/copyright

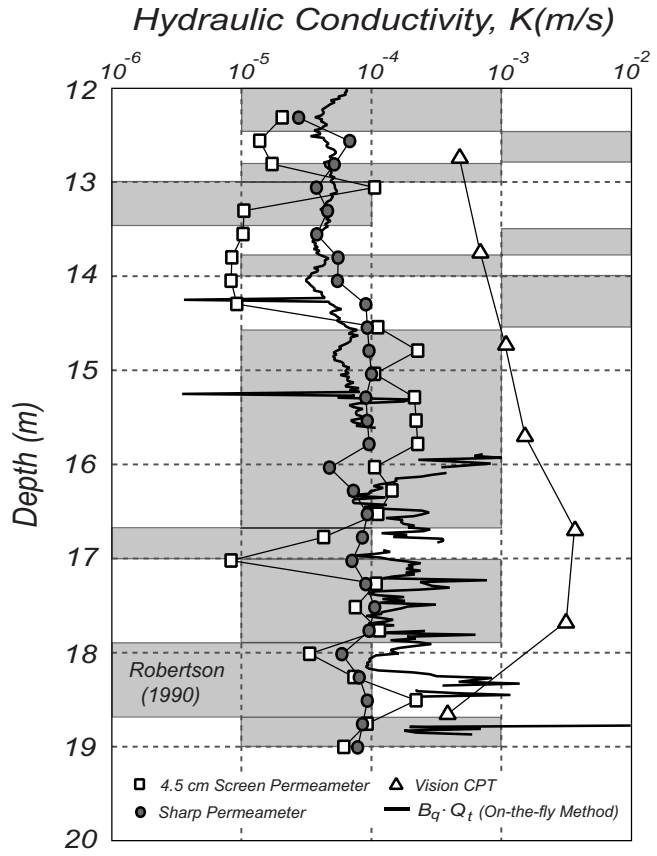

Fig. 10. Hydraulic conductivity measurements determined by in situ permeameter tests [4.5 cm length screen (squares) and sharp tip (circles)] and soil classifications [shade rectangle Robertson (1990) and triangles (VisCPT)] versus depth at the GEMS, Kansas. Hydraulic conductivity estimates determined from data pairs B_q-Q_t (solid line) [Eq. (9)].

Profiles

Another method of determining hydraulic conductivity profiles is in using correlations with soil classification schemes (Robertson 1990) and VisCPT, and in then linking these with quantitative estimates of hydraulic conductivity. Profiles of hydraulic conductivity determined from the large tip and sharp tip permeameters, and from on-the-fly, and soil classification predictions, are shown in Fig. 10. Negative magnitudes of excess pore pressures result in inadmissible predictions of hydraulic conductivity for estimation using B_q-Q_t and the pore pressure model cannot accommodate negative pore pressures. Magnitudes of hydraulic conductivity, K, predicted directly from $K_D=1/B_qQ_t$, were compared with the independent permeameter-measured profiles and extended to examine the traditional uCPT classification charts (Robertson 1990) and direct observation from high-quality VisCPT. Estimates of hydraulic conductivity using the ensemble suite of metrics, B_q-Q_t, are within two orders of magnitude of the estimates, $10^{-4}-10^{-5}$ m/s, especially in the sand and gravel layers below 12 m depth. The estimates from B_q-Q_t provide higher and scattered estimates, especially below 16 m depth, where measured induced pore pressure magnitudes are small. In this presumed higher hydraulic conductivity zone, induced pore pressures dissipate as quickly as they are developed in the penetration process. uCPT classification charts (Robertson 1990) provide values (filled rectangles) of 10^{-4} m/s over much of the profile (Fig. 10). The estimates from B_q-Q_t are uniformly lower than those evaluated from the soil classification method (Robertson 1990) in the upper layers (12–16 m depth), but yield close and consistent evaluations of hydraulic conductivity in the lower layer (16–19 m depth). The magnitudes of hydraulic conductivity from VisCPT (triangles in Fig. 10) are much larger than the other results. The larger differences are likely due to both inaccuracies in the Hazen formula (Hazen 1930) and the visual resolution of finer soil particles in a coarser particle matrix—correspondingly, these estimates may be considered as an upper bound—lager than actual values. The in situ permeameter test data provide the most reliable measurements of hydraulic conductivity, determined for influences of penetration-induced disturbance using two fabricated probe tips from adjacent uCPT boreholes (OTF #4). The predictions of hydraulic conductivity recovered from magnitudes of B_q-Q_t are higher than those independently measured by permeameter, especially below a depth of 16 m. However, these predictions and measurements from the sharp tip are consistently closer in the zone between 12 and 16 m, as illustrated in Fig. 10. The consistency between estimates recovered from B_q-Q_t and the sharp permeameter is taken as reasonable predictions of the hydraulic conductivity. These comparisons indicate that uCPT predictions of hydraulic conductivity from soundings (OTF #4) exhibit close agreement with those measured from in situ permeameter tests below 12 m. In particular, measurements of hydraulic conductivity from the sharp tip permeameter test are closest to predictions recovered from the pair B_q-Q_t, as illustrated in Fig. 10. The predictions from the larger tip, although not so close as for the sharp tip, exhibit a similar trend. The predictions yielded by the data pair B_q-Q_t provide the most robust evaluation in this comparison, as apparent in Fig. 10. These show strong correlation between the predicted hydraulic conductivity K values and those measured by the permeameters, as apparent in Fig. 10.

Conclusion

Profiles of hydraulic conductivity are measured at the GEMS site through the deployment of direct-push permeameters of two different configurations—one with a standard CPT-like tip, and the second with a thin tapered tip to minimize tip-local disturbance. Measurements of hydraulic conductivity were consistent between the closely correlated suite of measurements using the two tips, suggesting that tip-local disturbance around a standard cone is not significant. Consequently, permeameter measurements taken through a standard penetrometer tip, or via on-the-fly or dissipation measurements, are expected to be representative of pristine hydraulic conductivity magnitudes.

The extensive suite of in situ permeameter measurements enabled benchmarking of a variety of methods of evaluating hydraulic conductivity from direct-push methods. These included on-the-fly methods using the uCPT metrics ($B_q-F_r-Q_t$), high-quality observations of soil structure (VisCPT), and correlations with soil classifications derived from uCPT measurements. The feasibility of on-the-fly methods to determine hydraulic conductivity requires that tip-local pore pressures are both steady, and partially drained. The condition of steady behavior is reached where penetration is continuous and uninterrupted. Cone metrics are shown to be capable of distinguishing the threshold between conditions of partial drainage and of undrained behavior. This is apparent where $B_qQ_t<0.2$, $F_rQ_t<2.0$ and $F_r<0.02$, and $B_q/F_r<0.8$, respectively.

Downloaded 15 Nov 2008 to 128.118.16.83. Redistribution subject to ASCE license or copyright; see http://pubs.asce.org/copyright

Where undrained data are excluded, the hydraulic conductivity profile may be determined from magnitudes of the induced tip-local pore pressures, where the data represent remarkably close agreement with the relation $K_D=1/B_qQ_t$, at the equivalent depth, as illustrated in Figs. 9(b) and 10. These analyses show that the relation $K_D=1/B_qQ_t$ exhibits promise as a practical means of accurate prediction of hydraulic conductivity within feasible ranges where the penetration response is both partially drained and steady. The results indicate the potential to directly recover hydraulic conductivity during active steady penetration and without arresting penetration and waiting for the pore pressure to dissipate.

Acknowledgments

This work is as a result of partial support to Derek Elsworth from the National Science Foundation under Grant No. CMS-04090002. This work was also supported by the Basic Research Project of the Korea Institute of Geoscience & Mineral Resources (KIGAM) funded by the ministry of Science and Technology of Korea. This support is gratefully acknowledged. The writers gratefully acknowledge the access to GEMS provided by Jim Butler of the Kansas Geological Survey. The efforts of Michael Fitzgerald, Seungcheol Shin, Youngsub Jung, and Jan Pantolin who assisted with the field measurements are appreciated.

Notation

The following symbols are used in this paper:

A_c = projected frontal area of cone [L^2];
A_n = cross-sectional area of load cell or shaft [L^2];
a = penetrometer radius [L];
a_n = area ratio of cone (A_n/A_c) [-];
B_q = dimensionless pore pressure ratio, $(p-p_s)/(q_t-\sigma_{v0})$ [-];
dV = volume change per unit time in tip process zone [L^3T^{-1}];
F_r = normalized friction factor, $f_s/(q_t-\sigma_{v0})$ [-];
f_s = magnitude of sleeve friction [FL^{-2}];
K = hydraulic conductivity [LT^{-1}];
K_D = dimensionless hydraulic conductivity, $(4K\sigma'_{v0})/(Ua\gamma_w)$ [-];
$K_D^{B_q-F_r}$ = dimensionless hydraulic conductivity determined from B_q-F_r data [-];
$K_D^{B_q-Q_t}$ = dimensionless hydraulic conductivity determined from B_q-Q_t data [-];
$K_D^{F_r-Q_t}$ = dimensionless hydraulic conductivity determined from F_r-Q_t data [-];
p = absolute pore fluid pressure (u_2)[FL^{-2}];
p_s = initial static fluid pressure (u_0)[FL^{-2}];
$p-p_s$ = excess pore pressure [FL^{-2}];
Q_t = normalized cone resistance, $(q_t-\sigma_{v0})/\sigma_{v0}$ [-];
q_c = measured cone resistance [FL^{-2}];
q_t = corrected cone resistance $q_c+(1-a_n)p$[FL^{-2}];
U = penetrometer penetration rate ;[LT^{-1}];
γ_w = unit weight of water [FL^{-3}];
σ_v = total vertical stress [FL^{-2}]; and
$\sigma_{v0}, \sigma'_{v0}$ = initial vertical stress and effective stress [FL^{-2}].

References

Bohling, G. C. (1999). "Evaluation of an induced gradient tracer test in an alluvial aquifer." Ph.D. dissertation, Univ. of Kansas, Lawrence, Kan.

Bohling, G. C., Zhan, X., Butler, J. J., and Zheng, L. (2002). "Steady-shape analysis of tomographic pumping tests for characterization of aquifer heterogeneities." *Water Resour. Res.*, 38(12), 1324–1340.

Burns, S. E., and Mayne, P. W. (1998). "Monotonic and dilatory pressure decay during piezocone tests in clay." *Can. Geotech. J.*, 35(6), 1063–1073.

Butler, J. J. (2002). "A simple correction for slug tests in small-diameter wells." *Ground Water*, 40(3), 303–307.

Butler, J. J. (2005). "Hydrogeological methods for estimation of hydraulic conductivity." *Hydrogeophysics*, Springer, The Netherlands, 23–58.

Butler, J. J., and Dietrich, P. (2004). "New methods for high-resolution characterization of spatial variations in hydraulic conductivity." *Int. Proc. Symp. on Hydrogeological Investigation and Remedial Technology*, National Central University, Jhongli, Taiwan, 42–55.

Butler, J. J., Healey, J. M., Zheng, L., McCall, G. W., and Schulmeister, M. K. (1999a). "Hydrostratigraphic characterization of unconsolidated alluvium with direct-push sensor technology." *Open-File Rep. No. 99–40*, Kansas Geological Survey, Denver.

Butler, J. J., McElwee, D. D., and Bohling, G. C. (1999b). "Pumping tests in networks of multilevel sampling wells: Motivation and methodology." *Water Resour. Res.*, 35(11), 3553–3560.

Cardenas, M. B., and Zlotnik, V. A. (2003). "A simple constant-head injection test for streambed hydraulic conductivity estimation." *Ground Water*, 41(6), 867–871.

Dejong, J. T., DeGroot, D. J., Yafrate, N. J., and Jakubowski, J. (2003). "Detection of soil layering using a miniature piezoprobe." *Proc., Soil and Rock America 2003*, Vol. 1, Cambridge, Mass., 1 Verlag Gluckauf Essen, Essen, Germany, 192–197.

Douglas, B. J., and Olsen, R. S. (1981). "Soil classification using electric cone penetrometer." *Proc., Cone Penetration Testing and Experience*, ASCE, New York, 209–227.

Elsworth, D. (1990). "Theory of partially drained piezometer insertion." *J. Geotech. Engrg.*, 116(6), 899–914.

Elsworth, D. (1993). "Analysis of piezocone dissipation data using dislocation methods." *J. Geotech. Engrg.*, 119(10), 1601–1623.

Elsworth, D., and Lee, D. S. (2005). "Permeability determination from on-the-fly piezocone sounding." *J. Geotech. Geoenviron. Eng.*, 131(5), 643–653.

Elsworth, D., and Lee, D. S. (2007). "Methods and limits of determining permeability from on-the-fly CPT sounding." *Geotechnique*, 57(8), 679–685.

Fetter, C. W. (1998). *Applied hydrogeology*, Prentice-Hall, Upper Saddle River, N.J.

Hazen, A. (1930). "Water supply." *American civil engineers handbook*, Wiley, New York.

Hryciw, R. D., Ghalib, A. M., and Raschke, S. A. (1998). "In-situ characterization by VisCPT." *Proc., 1st. Int. Conf. on Site Characterization (ISC98)*, Balkema, Rotterdam, The Netherlands, 1081–1086.

Hryciw, R. D., Shin, S., and Ghalib, A. M. (2003). "High resolution site characterization by VisCPT with application to hydrogeology." *Proc., Soil and Rock America 2003*, Vol. 1, Cambridge, Mass. Verlag Gluckauf Essen, Essen, Germany, 334–339.

Lunne, T., Robertson, P. K., and Powell, J. J. M. (1997). *Cone penetration testing in geotechnical practice*, Blackie Academic and Processional, London.

McCall, G. W., Butler, J. J., Healey, J. M., Lanier, A. A., Sellwood, S. M., and Garnett, E. J. (2002). "A dual-tube direct-push method for vertical profiling of hydraulic conductivity in unconsolidated formations." *Environ. Eng. Geosci.*, 8(2), 75–84.

McElwee, D. D., Butler, J. J., and Healey, J. M. (1991). "A new sampling system for obtaining relatively undisturbed cores of unconsolidated

Downloaded 15 Nov 2008 to 128.118.16.83. Redistribution subject to ASCE license or copyright; see http://pubs.asce.org/copyright

coarse sand and gravel." *Ground Water Monit. Rev.*, 11(3), 182–191.
Mitchell, J. K., and Brandon, T. L. (1998). "Analysis and use of CPT in earthquake and environmental engineering." *Geotechnical site characterization*, Vol. 1, Balkema, Rotterdam, The Netherlands, 69–96.
Olsen, R. S. (1994). "Normalization and prediction of geotechnical properties using the cone penetrometer test." *Technical Rep. No. GL-94-29*, U.S. Army Corps of Engineers, Vicksburg, Miss.
Ostermeier, R. M., Pellerier, J. H., Winker, C. D., and Nicholson, J. W. (2001). "Trends in shallow sediment pore pressures—Deepwater Gulf of Mexico." *SPE/IACE Drilling Conference*, Amsterdam, The Netherlands, Society of Petroleum Engineering SPE/IADC 67772.
Raschke, S. A., and Hryciw, R. D. (1997). "Vision cone penetrometer (VisCPT) for direct subsurface soil observation." *J. Geotech. Geoenviron. Eng.*, 123(11), 1074–1076.
Robertson, P. K. (1990). "Soil classification using the cone penetration test." *Can. Geotech. J.*, 27(1), 151–158.
Robertson, P. K., Campanella, R. G., Gillespie, D., and Greig, J. (1986). "Use of piezometer cone data." *Proc., ASCE Spec. Conf. In-Situ '86: Use of In-Situ Tests in Geotechnical Engineering*, ASCE, Blacksburg, Va., 1263–1280.
Robertson, P. K., Sully, J. P., Woeller, D. J., Lunne, T., Powell, J. J. M., and Gillespie, D. G. (1992). "Estimating coefficient of consolidation from piezocone tests." *Can. Geotech. J.*, 29(4), 539–550.
Schulmeister, M. K., Butler, J. J., Healey, J. M., Zheng, L., Wysocki, D. A., and McCall, G. W. (2003a). "Direct-push electrical conductivity logging for high-resolution hydrostratigraphic characterization." *Ground Water Monit. Rem.*, 23(5), 52–62.
Schulmeister, M. K., Healey, J. M., Butler, J. J., and McCall, G. W. (2003b). "Direct-push geochemical profiling for assessment of inorganic chemical heterogeneity in aquifers." *J. Contam. Hydrol.*, 69(3–4), 215–232.
Sellwood, S. M., Healey, J. M., Birk, S. R., and Butler, J. J. (2005). "Direct-push hydrostratigraphic profiling." *Ground Water*, 43(1), 19–29.
Shin, S., and Hryciw, R. D. (2004). "Wavelet analysis of soil mass images for particle size determination." *J. Comput. Civ. Eng.*, 18(1), 19–27.
Whittle, A. J., Sutabutr, T., Germaine, J. T., and Varney, A. (2001). "Prediction and interpretation of pore pressure dissipation for a tapered piezoprobe." *Geotechnique*, 51, 601–617.

Downloaded 15 Nov 2008 to 128.118.16.83. Redistribution subject to ASCE license or copyright; see http://pubs.asce.org/copyright